ON THE APPLICATION OF THE HIGHER ORDER VIRTUAL ARRAY CONCEPT FOR SMALL ANTENNA ARRAYS

Ulrich Engel, Manfred Okum

Fraunhofer Institute for Communication, Information Processing and Ergonomics
Department Sensor Data and Information Fusion
ulrich.engel@fkie.fraunhofer.de, manfred.okum@fkie.fraunhofer.de

ABSTRACT

Recently, the fourth order virtual array concept ($q = 2$) has been extended to an arbitrary even order $m = 2q$ with $q \geq 2$. The intention of this paper is to investigate the direction finding performance related to GPS based on $4th$, $6th$ and $8th$ order processing methods compared to common $2nd$ order array processing methods. The presented results are based on real measurement data which has been recorded with our GPS antenna array (IKARUS) and our 8-channel recording system (ECHSE). We have used a 3-element antenna array because it is the smallest possible planar circular antenna. Additionally, the 3-element configuration exhibits useful properties regarding the virtual sensor positions.

1. INTRODUCTION

Controlled Reception Pattern Antennas (CRPA) can be used for GPS to mitigate both intentional and unintentional RF interferences. Many adaptive beamforming algorithms are described in the literature that estimate the space or space-time filter coefficients, usually known as Space-Time Adaptive Processing (STAP). A detailed description with numerous examples for space-time adaptive processing is given in [1]. Further information on GPS and interference mitigation algorithms can be found in [2, 3, 4, 5, 6]. More advanced space-time preprocessors generate a different space-time filter for each GPS satellite. As a result, these preprocessors require an accurate and reliable estimate of the direction of arrival (DOA) for each GPS satellite in view. The DOA information can be either obtained from an inertial measurement unit (IMU) or is estimated using array processing methods. Since we are interested in a series connection unit that requires no information from the GPS receiver we estimate the satellite DOA with our antenna array. However, GPS antennas have to be small due to cost and size limitations. These constraints limit the number of antenna elements and the performance in practical applications. But, the virtual array (VA) concept allows us to increase the number of elements, also called virtual sensors, without increasing the physical size of the antenna. The VA concept is based on Higher-Order-Statistics (HOS) and has been described in [7]. In the past, a couple of papers have been written on the application of Higher-Order-Statistics, e.g. [8, 9, 10, 11, 12, 13]. Recently, the resolution enhancement by HOS for small planar arrays has been studied in [14, 15]. However, little has been published on GPS DOA estimation using the VA concept for small antenna arrays. Especially, the VA concept combined with unknown satellite doppler frequency, i.e. without a-priori information, has not been investigated. Therefore, the paper is focused on the influence of the satellite doppler frequency and the received signal power on the DOA estimation performance. In this context, we have studied the differences between $2nd$, $4th$, $6th$ and $8th$-order array processing methods.
Section 2 describes the measurement equipment used for the analysis. In Section 3 and Section 4 the VA concept and the partial despreading procedure are discussed. Section 5 summarizes the DOA estimation results for the indoor and outdoor measurements.

2. MEASUREMENT EQUIPMENT

We have used our 7-element GPS antenna IKARUS[1] for the measurements. But only 3 channels of the 7-element antenna were selected for the following analyses. A picture showing the front and back of the IKARUS antenna is given in Figure 1. All measurements have been recorded using our ECHSE[2] system with a bandwidth of 5 MHz, which is sufficient for the processing of the GPS C/A-Code. The prototype of the ECHSE system has been developed in cooperation with Schönhofer Sales and Engineering GmbH. A valuable feature of the ECHSE system is the phase-coherent recording capability with up to 30 MHz signal bandwidth in real-time[3] [16].

Figure 1: 8-channel recording system ECHSE (left) and 7-element GPS antenna IKARUS (right).

During the outdoor measurements we have mounted the IKARUS antenna in a horizontal position. The position facilitated the reception of all GPS satellites in view. However, we have not calibrated the orientation of our antenna, because for our application it is not necessary to estimate the DOA with respect to a certain reference frame.
The indoor measurements have been carried out in a small anechoic chamber. The dimensions of the anechoic chamber are $2.00 \times 4.00 \times 4.00$ m and the attenuation at the GPS L1

[1] IKARUS: Intelligentes kleines Array zur Richtungsschätzung und Störunterdrückung.

[2] ECHSE: Eight Channel Data Recorder and Single Replay

[3] The ECHSE system has been awarded the Best Paper Award at the 15^{th} VIP-Congress 2010 in Munich.

frequency is approximately 30 dB, which is sufficient to mitigate multipath effects. The IKARUS antenna was mounted in a vertical position facing towards the Tx-antenna at an elevation angle $\varphi = 90^o$.

3. HIGHER ORDER VIRTUAL ARRAY CONCEPT

The complex baseband output at the ith antenna element can be written as [17]:

$$z_i = \sum_{k=1}^{M} b_k e^{j2\pi \mathbf{r}_i^T \mathbf{u}_k/\lambda} + n_i \tag{1}$$

with $i = 1 \ldots N$, N = size of antenna array, b_k denotes the complex amplitude of the kth source, $\mathbf{u}_k = (u_k, v_k, w_k)$ specifies the direction of the kth plane wave impinging on the array, $\mathbf{r}_i = (x_i, y_i, 0)^T$ describes the element positions of the planar antenna array, λ = signal wavelength and n_i = uncorrelated unit variance gaussian noise. Finally, in vector notation the array data snapshot is given by:

$$\mathbf{z} = \mathbf{A}\mathbf{b} + \mathbf{n} \tag{2}$$

with $\mathbf{A} = (\mathbf{a}(\mathbf{u_1}), \ldots, \mathbf{a}(\mathbf{u_M}))$ and $\mathbf{a}_i = e^{j2\pi(x_i u + y_i v)/\lambda}$.
In order to demonstrate the performance characteristics of the different HOS based array processing methods we have chosen the beamforming method. But other methods are also possible, e.g. MUSIC or CAPON [18, 19]. Finally, the DOA has been determined by:

$$\text{DOA} = \arg\max[\mathbf{a}(\mathbf{u})^H \mathbf{C}_{2q,l} \mathbf{a}(\mathbf{u})] \tag{3}$$

with $\mathbf{C}_{2q,l}$ = circular covariance matrix being defined in the following paragraph. The Higher Order Virtual Array Concept allows us to describe the increasing resolution capabilities of $2qth$ order array processing methods. The $2qth$ ($q \geq 1$) order array processing methods exploit the information contained in the covariance matrix. The matrix entries are the $2qth$ circular cumulants of the input data and are defined as:

$$Cum[z_{i_1}(t), \ldots, z_{i_q}(t), z_{i_{q+1}}(t)^*, \ldots, z_{i_{2q}}(t)^*] \tag{4}$$

with $(1 \leq i_j \leq N), (1 \leq j \leq 2q)$ and * corresponds to complex conjugation. In [7] it is shown that the $\mathbf{C}_{2q,l}$ covariance matrix can be rewritten as:

$$\begin{aligned} \mathbf{C}_{2q,l}(z) &\approx \sum_{i=1}^{P} c_{2q,m_i} [\mathbf{a}^{\otimes l} \otimes \mathbf{a}^{*\otimes(q-l)}] \times [\mathbf{a}^{\otimes l} \otimes \mathbf{a}^{*\otimes(q-l)}]^\dagger \\ &+ \eta_2 V \delta(q-1) \end{aligned} \tag{5}$$

with $c_{2q,m_i} = Cum[m_{i_1}, \ldots, m_{i_q}, m^*_{i_{q+1}}, \ldots, m^*_{i_{2q}}]$ is the $2qth$ order cumulant, $\dagger$ = conjugate transpose operator, η_2 = mean power of noise per sensor, $V = N \times N$ spatial coherence matrix, $\delta()$ = Kronecker symbol, $\otimes$ = Kronecker product and $\mathbf{a}^{\otimes l}$ = the vector defined by $\mathbf{a}^{\otimes l} = \mathbf{a} \otimes \mathbf{a} \otimes \ldots \otimes \mathbf{a}$ with the number of Kronecker products equal to $l - 1$. For detailed information on the parameter q and l we refer the reader to the reference section, e.g. [7].
In order to reduce the computational complexity we have used the following expressions for the estimation of the covariance matrix $\mathbf{C}_{2q,l}(z)$. In fact, these expressions are estimators of $2qth$ order moments instead of $2qth$ order cumulants, but the results of our analysis have confirmed this choice. The general form of the used statistical estimators is given by:

$$\hat{\mathbf{C}}_{2q,l}(z) = \frac{1}{K} \sum_{k=1}^{K} [\mathbf{z}_k^{\otimes l} \otimes \mathbf{z}_k^{*\otimes(q-l)}] \times [\mathbf{z}_k^{\otimes l} \otimes \mathbf{z}_k^{*\otimes(q-l)}]^\dagger \tag{6}$$

From equation (6) we obtain the following estimators for the covariance matrix (K = number of snapshots and $\bar{\mathbf{z}}$ = complex conjugation of $\mathbf{z}$):

- $q = 1$: 2nd-order moment

$$\hat{\mathbf{C}}_{\mathbf{2}} = \frac{1}{K} \sum_{k=1}^{K} \mathbf{z}_k \mathbf{z}_k^H \tag{7}$$

- $q = 2$: 4th-order moment

$$\hat{\mathbf{C}}_{\mathbf{41}} = \frac{1}{K} \sum_{k=1}^{K} (\mathbf{z}_k \otimes \bar{\mathbf{z}}_k)(\mathbf{z}_k \otimes \bar{\mathbf{z}}_k)^H \tag{8}$$

$$\hat{\mathbf{C}}_{\mathbf{42}} = \frac{1}{K} \sum_{k=1}^{K} (\mathbf{z}_k \otimes \mathbf{z}_k)(\mathbf{z}_k \otimes \mathbf{z}_k)^H \tag{9}$$

- $q = 3$: 6th-order moment

$$\hat{\mathbf{C}}_{\mathbf{62}} = \frac{1}{K} \sum_{k=1}^{K} (\mathbf{z}_k \otimes \mathbf{z}_k \otimes \bar{\mathbf{z}}_k)(\mathbf{z}_k \otimes \mathbf{z}_k \otimes \bar{\mathbf{z}}_k)^H \tag{10}$$

$$\hat{\mathbf{C}}_{\mathbf{63}} = \frac{1}{K} \sum_{k=1}^{K} (\mathbf{z}_k \otimes \mathbf{z}_k \otimes \mathbf{z}_k)(\mathbf{z}_k \otimes \mathbf{z}_k \otimes \mathbf{z}_k)^H \tag{11}$$

- $q = 4$: 8th-order moment

$$\hat{\mathbf{C}}_{\mathbf{82}} = \frac{1}{K} \sum_{k=1}^{K} (\mathbf{z}_k \otimes \mathbf{z}_k \otimes \bar{\mathbf{z}}_k \otimes \bar{\mathbf{z}}_k)(\mathbf{z}_k \otimes \mathbf{z}_k \otimes \bar{\mathbf{z}}_k \otimes \bar{\mathbf{z}}_k)^H \tag{12}$$

$$\hat{\mathbf{C}}_{\mathbf{83}} = \frac{1}{K} \sum_{k=1}^{K} (\mathbf{z}_k \otimes \mathbf{z}_k \otimes \mathbf{z}_k \otimes \bar{\mathbf{z}}_k)(\mathbf{z}_k \otimes \mathbf{z}_k \otimes \mathbf{z}_k \otimes \bar{\mathbf{z}}_k)^H \tag{13}$$

$$\hat{\mathbf{C}}_{\mathbf{84}} = \frac{1}{K} \sum_{k=1}^{K} (\mathbf{z}_k \otimes \mathbf{z}_k \otimes \mathbf{z}_k \otimes \mathbf{z}_k)(\mathbf{z}_k \otimes \mathbf{z}_k \otimes \mathbf{z}_k \otimes \mathbf{z}_k)^H \tag{14}$$

Equation (5) demonstrates that in general the virtual array configurations differ in shape and number of virtual sensors depending on q and l. According to [7], the corresponding steering vector for the virtual array configuration is given by:

$$\begin{aligned} [\mathbf{a}^{\otimes l} \otimes \overline{\mathbf{a}}^{\otimes(q-l)}]_i &= \exp\left\{ j2\pi \left[\left(\sum_{j=1}^{l} x_{k_j} - \sum_{u=1}^{q-l} x_{k_{l+u}} \right) u \right.\right. \\ &\left.\left. + \left(\sum_{j=1}^{l} y_{k_j} - \sum_{u=1}^{q-l} y_{k_{l+u}} \right) v \right] / \lambda \right\} \end{aligned} \tag{15}$$

with $i =$ denoting the virtual sensor.

Some of these N^q virtual sensor positions will usually coincide. This redundancy can be used to decrease computational costs. The maximum number of non-redundant virtual sensors associated with the VA can be easily calculated. For the smallest planar antenna array with 3-elements the values are summarized in Table 1 (see also [20]). The corresponding virtual sensor positions are shown in Figure 2.

q=2		q=3		q=4		
l=2	l=1	l=3	l=2	l=4	l=3	l=2
6	7	10	12	15	18	19

Table 1: Maximum number of non-redundant virtual sensors based on 3-element planar array.

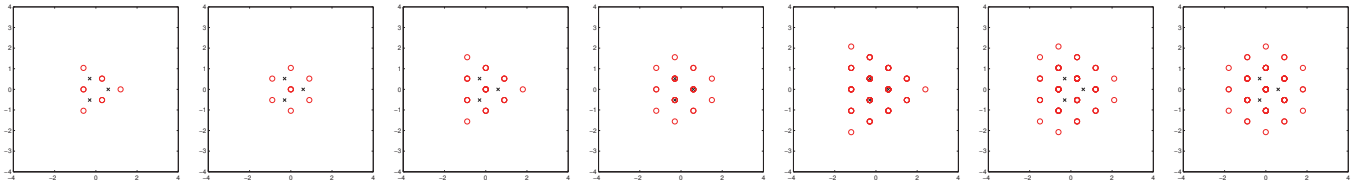

(a) $N_{l=2}^{q=2} = 6$ (b) $N_{l=1}^{q=2} = 7$ (c) $N_{l=3}^{q=3} = 10$ (d) $N_{l=2}^{q=3} = 12$ (e) $N_{l=4}^{q=4} = 15$ (f) $N_{l=3}^{q=4} = 18$ (g) $N_{l=2}^{q=4} = 19$

Figure 2: Virtual array configurations based on 3-element planar antenna depending on q and l.

4. DOA ESTIMATION BY PARTIAL DESPREADING

In order to determine the DOA of the GPS satellite it is necessary to correlate and integrate the received C/A-Code signal at each element of the antenna array with a local replica of the C/A-Code. This correlation process will be successful if the doppler frequency of the GPS signal is exactly known. In general, the doppler frequency is not known beforehand and the correlation process will usually fail. But, instead of correlating with a complete pseudo random noise (PRN) sequence of $Q = 1023$ chips we can split the C/A-Code PRN sequence into $S = 2, 4, 8, 16$ or 32 subblocks of length $Q = 512, 256, 128, 64$ or 32 chips [5]. The more subblocks are used the less sensitive is the partial despreading process against a doppler frequency mismatch. However, with every bisection of the PRN-sequence we loose 3 dB correlation gain. Fortunately, this disadvantage is normally irrelevant because even a correlation gain of 18 dB is often sufficient for the DOA estimation. For each subblock we form a correlation matrix based on equation (6), which can be slightly modified to account additionally for the cyclostationarity of the C/A-Code signal. Afterwards, the outputs of all S correlation matrices can be averaged as:

$$\hat{\mathbf{C}}_{averaged} = \frac{1}{S}\sum_{s=0}^{S-1}\hat{\mathbf{C}}_s\hat{\mathbf{C}}_s^H \tag{16}$$

5. DOA ESTIMATION RESULTS

At first we present the results from the indoor measurements. We have analysed the performance of the DOA estimation by changing the power level of the C/A-Code, i.e. C/N_o values in the range $30 - 52$ dBHz. The doppler frequency of the GPS signal was fixed with $f_d = 0$. The integration time of the correlation process was set to $T = 1$ msec and the number of subblocks was $S = 1$.

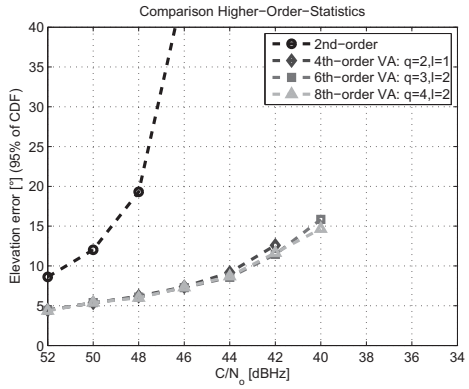

Figure 3: Results of $2nd$, $4th$, $6th$ and $8th$ order processing for complete virtual arrays with variable C/N_o.

Figure 3 shows the elevation error based on a Monte-Carlo analysis (500 runs). The results correspond to the 95% value of the cumulative distribution function (CDF)[4]. From Figure 3 it is obvious that the $2nd$ order statistic performs worst. The results for the Higher-Order-Statistics, i.e. $4nd$, $6th$ and $8th$ are quite similar, with small differences for lower C/N_o values.
Figure 4 illustrates the differences between non-redundant and redundant virtual arrays. First of all, we can see that the non-redundant virtual arrays show usually the same performance as the redundant VAs. Furthermore, for low C/N_o values we observe that the VAs with less non-redundant virtual sensor positions, e.g. $\text{VA}_{l=2}^{q=2}$, $\text{VA}_{l=3}^{q=3}$, $\text{VA}_{l=4}^{q=4}$ perform slightly worse.

In a second step we kept the power level constant at $C/N_o = 50$ dBHz and changed the doppler frequency of the GPS signal. The doppler frequency was in the range $0 - 6000$ Hz with a stepsize of 500 Hz. This time we applied the partial-despreading method [5] because we assumed that the doppler frequency of the GPS signal was unknown. We used $S = 4$ subblocks with a length of $Q = 256$ chips. In order to compensate for the correlation loss due to the partial despreading, we have increased the integration time to $T = 5$ msec. Figure 5 illustrates that the results from $2nd$ order statistics are unusable even for a $C/N_o = 50$ dBHz[5]. However, the performance gain using Higher-Order-Statistics is quite remarkable. If we increase the number of subblocks, the DOA estimation would work for even higher doppler frequencies. The results for non-redundant and redundant VAs are presented in Figure 6.

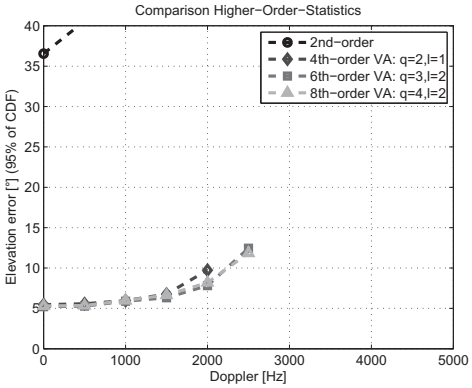

Figure 5: Results of $2nd$, $4th$, $6th$ and $8th$ order processing for complete virtual arrays with variable doppler frequency.

[4]The standard deviation is commonly used to evaluate data sets. However, the standard deviation is not an appropriate measure if there are outliers in the data.

[5]The signal strength of the GPS signal is usually in the range $40 - 52$ dBHz (at the Earth surface).

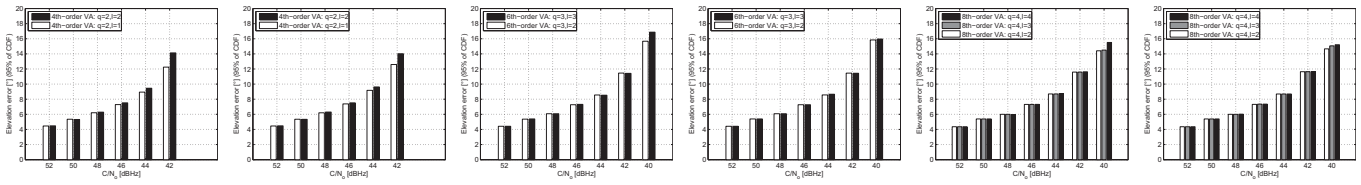

(a) $N = 6, 7$ (b) $N = 9$ (c) $N = 10, 12$ (d) $N = 27$ (e) $N = 15, 18, 19$ (f) $N = 81$

Figure 4: Non-redundant vs. redundant ($N = 9, 27, 81$) VAs (for variable C/N_o): $4th$ (a)-(b), $6th$ (c)-(d) and $8th$ (e)-(f).

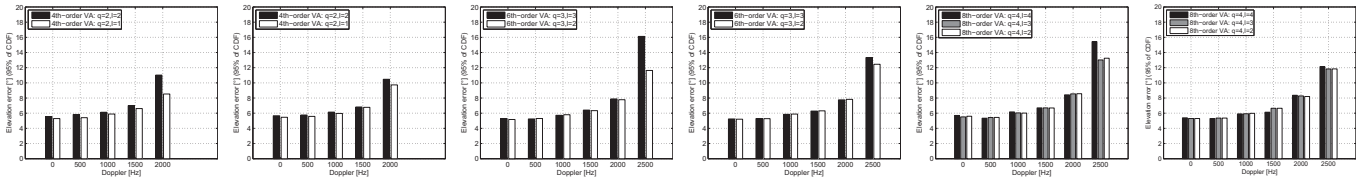

(a) $N = 6, 7$ (b) $N = 9$ (c) $N = 10, 12$ (d) $N = 27$ (e) $N = 15, 18, 19$ (f) $N = 81$

Figure 6: Non-redundant vs. redundant ($N = 9, 27, 81$) VAs (for variable doppler): $4th$ (a)-(b), $6th$ (c)-(d) and $8th$ (e)-(f).

As mentioned in Section 2, we have also carried out several outdoor measurements with the IKARUS antenna. The aim was to show the performance of the statistical estimators given in Section 3 and to verify the used measurement setup. The satellite constellation at the beginning of the outdoor measurements is illustrated in Figure 7.

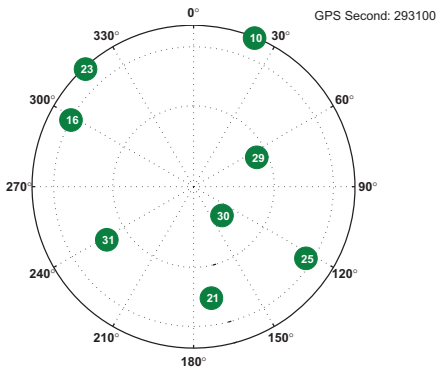

Figure 7: Satellite constellation at the beginning of the outdoor measurements.

During the recording up to 8 GPS satellites were visible. However, due to shadowing effects and low elevation angles we could not acquire the satellites with PRN number 10 and 23. The corresponding Correlation-Peak-to-Peak-Ratios (CPPR)[6] of the acquisition process are listed in Table 2.

PRN	10	16	21	23	25	29	30	31
CPPR	0.7	7.5	7.2	0.3	6.9	9.4	11.3	8.6

Table 2: Correlation-Peak-to-Peak-Ratios (CPPR) in [dB].

In Figure 8 we have plotted the beamforming pattern for the GPS satellite corresponding to PRN 30, which has the best CPPR value of all visible satellites in the szenario (see Table 2). The C/N_o value of the satellite was not determined, but based on daily experiences the C/N_o value for this satellite was in the range of $48-50$ dBHz. Moreover, we see that the antenna was not calibrated northwards (as mentioned previously), because the maximum of the beamforming pattern does not coincide with the DOA of PRN 30 in Figure 7. It can be determined that the beam becomes narrower the higher the order of the virtual array is. After eliminating all redundant virtual sensor positions we see that the beam becomes even narrower compared to the complete virtual array (see Figure 9). This is due the fact, that the redundant sensor positions function like a tapering of the antenna aperture. This effect leads to a broadening of the main lobe. Additionally, we can observe from the figures that the proposed simplified estimators for the covariance matrices operate successfully.

[6]The Correlation-Peak-to-Peak-Ratio is the ratio between the first and second maximum of the correlation process (acquisition), e.g. parallel code phase search.

6. CONCLUSIONS

The presented results show that it is difficult to obtain a reliable DOA estimate with the 3-element antenna array based on $2nd$ order statistics. Better results could be achieved if we use longer integration times for the correlation process. However, we have already used an integration time $T = 5$ msec, which is five times the C/A-Code period. Much longer integration times are probably not practicable in a majority of applications. The HOS based methods perform significantly better in this context. Even with a short integration time of $T = 1$ msec we could obtain reliable DOA estimates based on Higher-Order-Statistics. The Monte-Carlo analyses show that the $4th$ order statistics achieve higher accuracy and increased robustness for low signal to noise ratios C/N_o. The same can be confirmed for the $6th$ and $8th$ order statistics compared to the $2nd$ order statistics. Furthermore, the Monte-Carlo analyses show that the $6th$ and $8th$ order statistics are more robust for low C/N_o values compared to the results based on $4th$ order statistics. The reason for this is most likely the higher number of virtual sensors. So far we did not determine the codephase of the C/A-Code during the DOA estimation process, i.e. we were not synchronized in time with the peak of the autocorrelation function of the C/A-Code. For future investigations we intend to exploit the codephase information from the C/A-Code and we plan to compare the performance of both approaches.

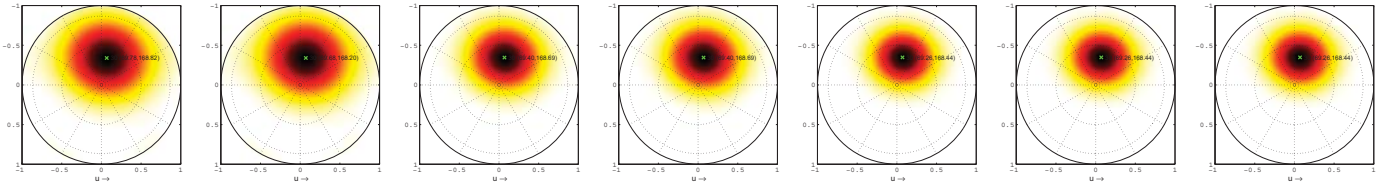

(a) $N_{l=2}^{q=2} = 9$ (b) $N_{l=1}^{q=2} = 9$ (c) $N_{l=3}^{q=3} = 27$ (d) $N_{l=2}^{q=3} = 27$ (e) $N_{l=4}^{q=4} = 81$ (f) $N_{l=3}^{q=4} = 81$ (g) $N_{l=2}^{q=4} = 81$

Figure 8: DOA beamforming pattern of GPS satellite (PRN 30) using all virtual sensors ($N = 3^q$).

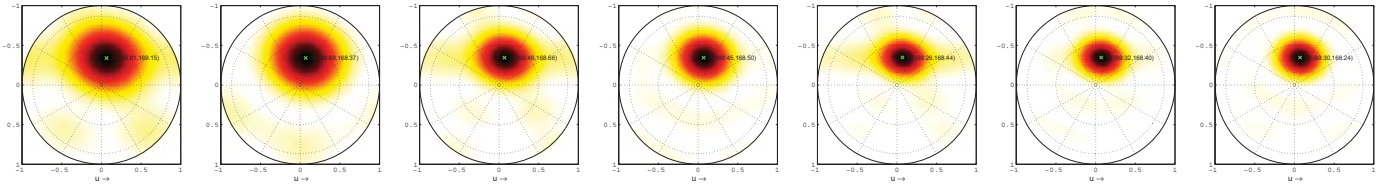

(a) $N_{l=2}^{q=2} = 6$ (b) $N_{l=1}^{q=2} = 7$ (c) $N_{l=3}^{q=3} = 10$ (d) $N_{l=2}^{q=3} = 12$ (e) $N_{l=4}^{q=4} = 15$ (f) $N_{l=3}^{q=4} = 18$ (g) $N_{l=2}^{q=4} = 19$

Figure 9: DOA beamforming pattern of GPS satellite (PRN 30) using non-redundant virtual arrays.

REFERENCES

[1] R. Klemm, *Applications of Space-Time Adaptive Processing*, IEE Radar, Sonar and Navigation Series 14, ISBN 0-85296-924-4, 2004.

[2] GPS Joint Program Office, *Navstar Global Positioning System - Interface Specification*, IS-GPS-200 Revision D, 07 December 2004.

[3] J. Spilker and B. Parkinson, *Global Positioning System: Theory and Applications*. American Institute of Aeronautics and Astronautics, Washington, 1996.

[4] E.D. Kaplan and C.J. Hegarty, *Understanding GPS Principles and Applications*. Artech House, 2005.

[5] M.D. Zoltowski, "Jam-Proof Area Deniable Propagation," Final Technical Report, October 2000.

[6] K. Borre and D.M. Akos, *A Software-Defined GPS and GALILEO Receiver*. Birkhäuser, 2007.

[7] P. Chevalier and L. Albera and A. Ferréol and P. Comon, "On the Virtual Array Concept for Higher Order Processing," IEEE Transactions on Signal Processing, Vol. 53, No. 4, April 2005.

[8] M.C. Dogan and J.M. Mendel, "Applications of Cumulants to Array Processing - Part I: Aperture Extension and Array Calibration," IEEE Transactions on Signal Processing, Vol. 43, No. 5, May 1995.

[9] M.C. Dagon and J.M. Mendel, "Applications of Cumulants to Array Processing - Part II: Non-Gaussian Noise Suppression," IEEE Transactions on Signal Processing, Vol. 43, No. 7, July 1995.

[10] E. Gönen and J.M. Mendel, "Applications of Cumulants to Array Processing - Part III: Blind Beamforming for Coherent Signals," IEEE Transactions on Signal Processing, Vol. 45, No. 9, September 1997.

[11] E. Gönen and J.M. Mendel and M.C. Dogan, "Applications of Cumulants to Array Processing - Part IV: Direction Finding in Coherent Signals Case," IEEE Transactions on Signal Processing, Vol. 45, No. 9, September 1997.

[12] T. Liu and J.M. Mendel, "Applications of Cumulants to Array Signal Processing - Part V: Sensitivity Issues," IEEE Transactions on Signal Processing, Vol. 47, No. 3, March 1999.

[13] E. Gönen and J.M. Mendel, "Applications of Cumulants to Array Signal Processing - Part VI: Polarization and Direction of Arrival Estimation with Minimally Constrained Arrays," IEEE Transactions on Signal Processing, Vol. 47, No. 9, March 1999.

[14] U. Nickel, "Resolution Enhancement By HOS for Small Planar Arrays," Sensor Array and Multichannel Signal Processing Workshop, 5th IEEE SAM2008, July 2008.

[15] U. Nickel, "Anwendung von höheren Momenten zur Erhöhung der Auflösung bei kleinen planaren Antennen," FKIE-Bericht Nr. 154, März 2008.

[16] U. Wessel, "ECHSE - Funksignale Breitbandig Aufzeichnen," Virtuelle Instrumente in der Praxis 2010, Begleitband zum 15. VIP-Kongress, p.198, SSE GmbH, October 2010, Munich.

[17] L.C. Godara, "Application of Antenna Arrays to Mobile Communications, Part II: Beam-Forming and Direction-of-Arrival Considerations," Proceedings of the IEEE, Vol. 85, No. 8, August 1997.

[18] R.O. Schmidt, "Multiple Emitter Location and Signal Parameter Estimation", IEEE Transactions on Antennas and Propagation, Vol. AP-34, No. 3, 1986.

[19] J. Capon, "High-resolution frequency-wave number spectrum analysis," Proc. IEEE, Vol. 57, pp. 1408-1418, 1969.

[20] L. Albera and A. Ferréol and P. Comon and P. Chevalier, "Blind Identification of Over-complete MixturEs of sources (BIOME)," Linear Algebra Appl., 2004.